Plasma enabled non-thermal phosphorization for nickel phosphide hydrogen evolution catalysts

Xiuqi Wu, [a] Yanru Guo, [a] Teng Wang, [a] Bingxue Sun, [a] Zhiliang Liu[a] , Yong Wu, [a] Shaojun Zhang, [a] Jie Zheng[a] and Xingguo Li*[a]*

Beijing National Laboratory of Molecular Sciences (BNLMS), College of Chemistry and Molecular Engineering, Peking University, Beijing 100871, China.

E-mail: xgli@pku.edu.cn, zhengjie@pku.edu.cn

1. Material preparation

1.1 Direct growth of $Ni(OH)_2$ nanosheets on Ni foam ($Ni(OH)_2$/NF) and conversion to NiO/NF

Ni foam is cleaned by ultrasonication successively in 6 M HCl, water and ethanol, and then dried under vacuum at 60 °C before used. In a typical synthesis, $Ni(NO_3)_2 \cdot 6H_2O$ (1 mmol), NH_4F (4 mmol) and urea (12 mmol) (All chemicals are of analytical grade purchased from J. K Chemicals and are used without further treatment.) are dissolved in 20 mL of deionized water. Next, the solution is transferred to a Teflon-lined autoclave reactor (25 mL). One piece of cleaned Ni foam (2 cm x 4 cm) with metallic sheen is then fully immersed in the solution and placed against the inner wall of the Teflon liner. The autoclave is subsequently sealed and heated to 120 °C, and maintained at this temperature for 16 h. After cooling to room temperature, the Ni foam turns into green, which is collected and thoroughly rinsed with deionized water and ethanol, and dried under vacuum at 60 °C. Then the green $Ni(OH)_2$/NF is annealed at 400 °C for 1 h with heating rate of 5 °C/min to produce NiO/NF, which shows a pale yellow colour.

1.2 Ni_2P/NF prepared by non-thermal plasma phosphorization.

The plasma treatment setup is illustrated in Figure 1a, which consists of a quartz tube furnace with an inductive coil placed in the upstream of the furnace. Plasma can be generated at low pressure (1-100 Pa) by 13.56 MHz radio frequency power input into the coil.

The NiO/NF sample is loaded into the centre of the furnace and red phosphorous (0.1 g) is placed upstream to the NiO/NF sample with a gap ~ 3 cm where the temperature is same as the NiO/NF sample. The tube furnace is first evacuated into 0.1 Pa with a rotary pump and is flushed with high purity Ar (99.999%) three times to remove oxygen and moisture. The red phosphorous and also the NiO/NF sample is heated to 250 °C at 15 °C/min in a mixture of Ar/H_2 flow (Ar 10 sccm and H_2 20 sccm) at pressure ~ 50 Pa. When the desired temperature is reached, plasma is ignited with input power of 120 W. A light yellow glow is able to extend to the NiO/NF region. The treatment time is 1 h. After treatment, the plasma is turned off and the system is cooled down to room temperature in the same Ar/H_2 flow. The average mass loading of Ni_2P is about 0.48 mg cm^{-2}, which was determined by weighting Ni foam before and after phosphorization using an analytical balance with a nominal precision of 0.01 mg. The bare Ni foam and $Ni(OH)_2$/NF samples are phosphorized through the same process.

2. Materials Characterization

2.1 Structural characterization

The structure and morphology of products are characterized by X-ray diffraction (XRD, Rigaku D/max 200 diffractometer, Cu Kα), scanning electron microscopy (SEM, ZEISS, Merlin Compact) and high-resolution transmission electron microscopy (HRTEM, JEM 2100F, 200 kV). For TEM observation, the Ni_2P nanosheets are removed from the Ni foam by sonication in ethanol for 30 min. Then a few drops of the suspension are casted onto TEM grids. The X-ray photoelectron spectroscopy (XPS) analysis is performed

on an AXIS-Ultra spectrometer (Kratos Analytical) using monochromatic Al Ka radiation (225 W, 15 mA, 15 kV). The binding energy at 284.6 eV of the C 1s is used as the reference for calibration.

2.2 Electrochemical characterization

The as-synthesized samples on Ni foam is directly used for electrocatalytic HER in acidic solution. All electrochemical measurements of the samples are performed at room temperature. The data is recorded using a CHI 660B electrochemical workstation (CHI Instruments, Inc., USA) in a standard three-electrode setup. The reference electrode is a saturated calomel electrode (SCE) and the counter electrode is a graphite rod. All the potentials reported in our work are converted to the reversible hydrogen electrode (RHE) scale.

The LSV is tested at a rate of 5 mV s^{-1} in a range from 0.002 to -0.3 V (vs RHE) and EIS is carried out under η = 65 mV with an amplitude of 2 mV. The electrochemically active surface areas of the catalysts are compared on a relative scale using the capacitance of the electrochemical double layer (C_{dl}) on the electrode-electrolyte interface at the non-Faradaic region (iC). Faradaic efficiency is determined by measuring the volume of gases generated on the working electrode chamber in galvanostatic condition. The volume of gas in the work electrode chamber can be determined with accuracy up to 0.1 cm^3 using a calibrated, adjustable U-shaped glass tube filled with water. The volume of gas is converted into moles using the ideal gas law.

Solar-driven water electrolysis is performed on a home-designed eletrolyzer made of poly(methyl methacrylate) with a commercial polycrystalline silicon solar cell. Commercial RuO_2 (from SigmaAldrich Co. Ltd.) is employed as OER catalyst, loaded on an 1cm^2 carbon cloth with a loading density of 2 mg cm^{-2}. These two electrodes are separated by a piece of Nafion membrane. The power density of irradiance is measured by a solar radiometer (Photoelectric Instrument of Beijing Normal University).

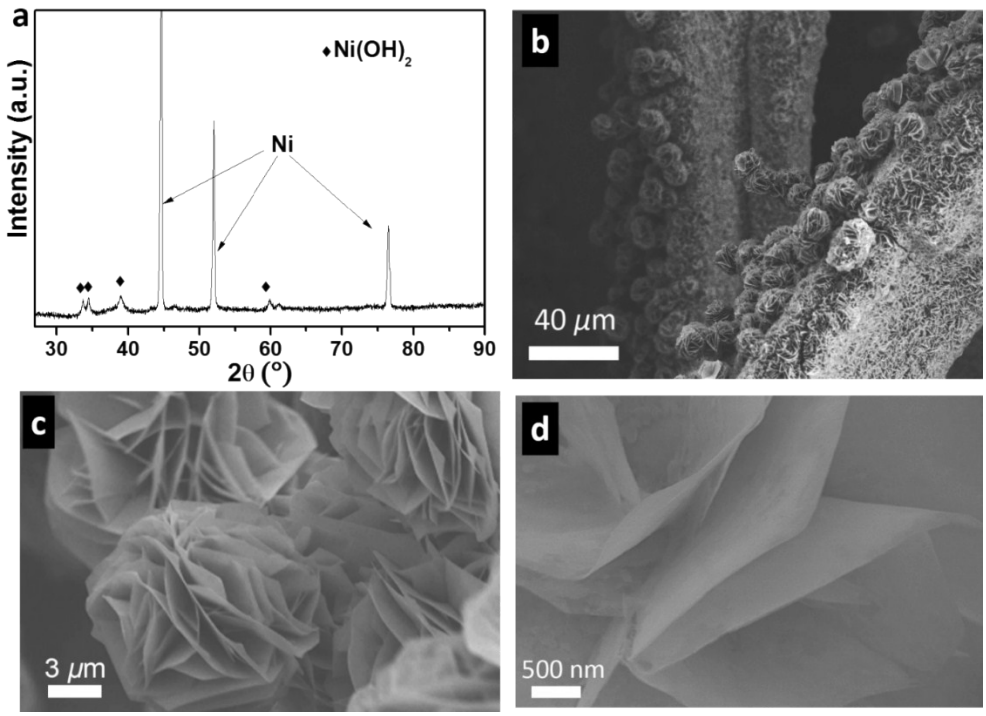

Fig. S1 Structural characterization of precursor $Ni(OH)_2$/NF. (a) XRD pattern. (b-d) SEM images at different scales.

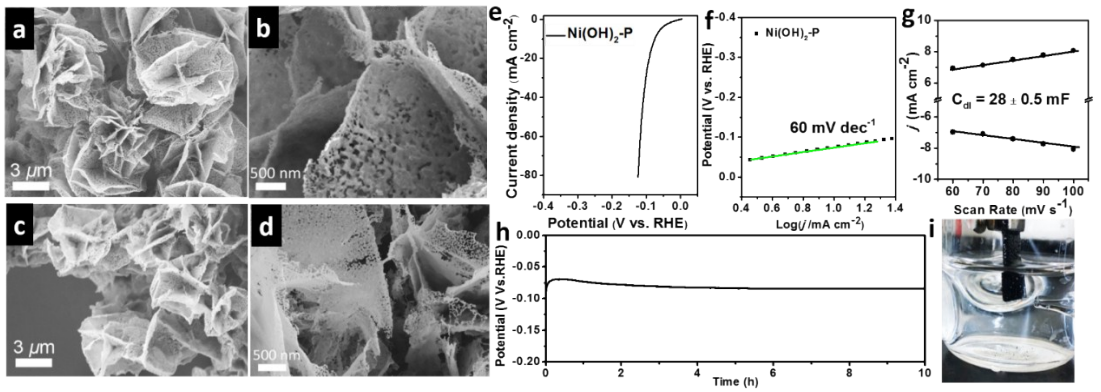

Fig. S2 Characterization of the HER catalyst $Ni(OH)_2$-P/NF. (a-d) SEM images of the $Ni(OH)_2$-P/NF before and after the galvanostatic electrolysis. (e-f) The Linear scanning polarization curve and the Tafel plots. (g) Current density as a function of scan rate for C_{dl} caculation. (h) The potential profiles of the electrolysis during a galvanostatic electrolysis for 10 h at 10 mA cm^{-2}. (i) A photograph of the working electrode after 10 h test, disintegration of the electrode is observed.

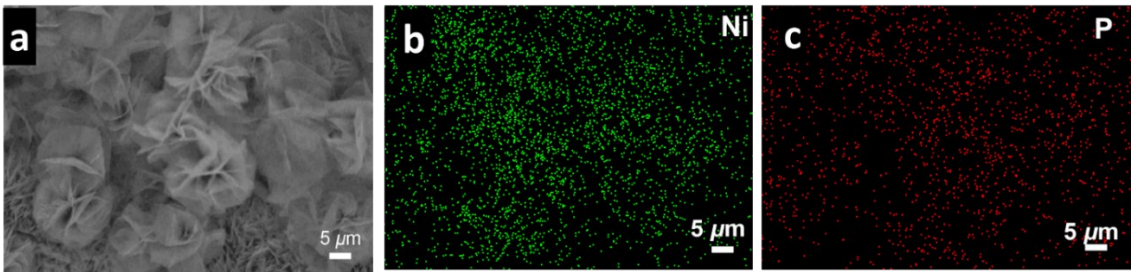

Fig. S3 (b)-(c) EDS spectrum of Ni_2P/NF in SEM of the corresponding region in pattern a.

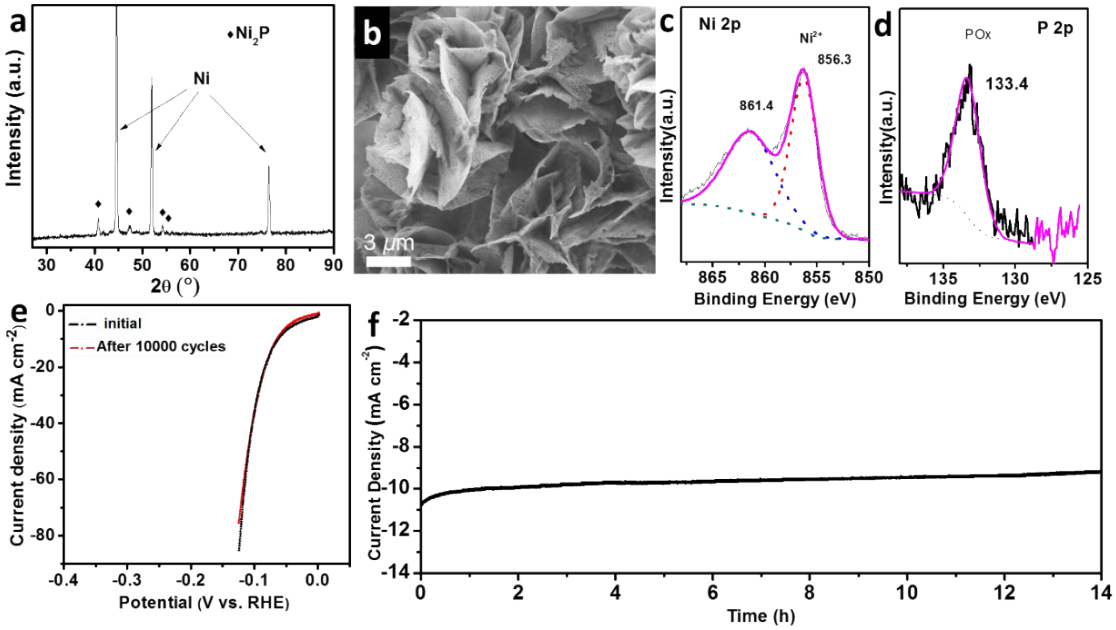

Fig. S4 (a-d)Structural characterization of Ni_2P/NF after galvanostatic measurement at different current density. (a) XRD patterns and (b) SEM images. (c-d) the XPS spectra. Further demonstration of the catalytic stability of Ni_2P/NF. (e) Linear polarization curves before and after 10,000 cyclic voltammetry cycles of Ni_2P/NF in 0.5 M H_2SO_4. (f) Potentiostatic measurement at an overpotential of 90 mV.

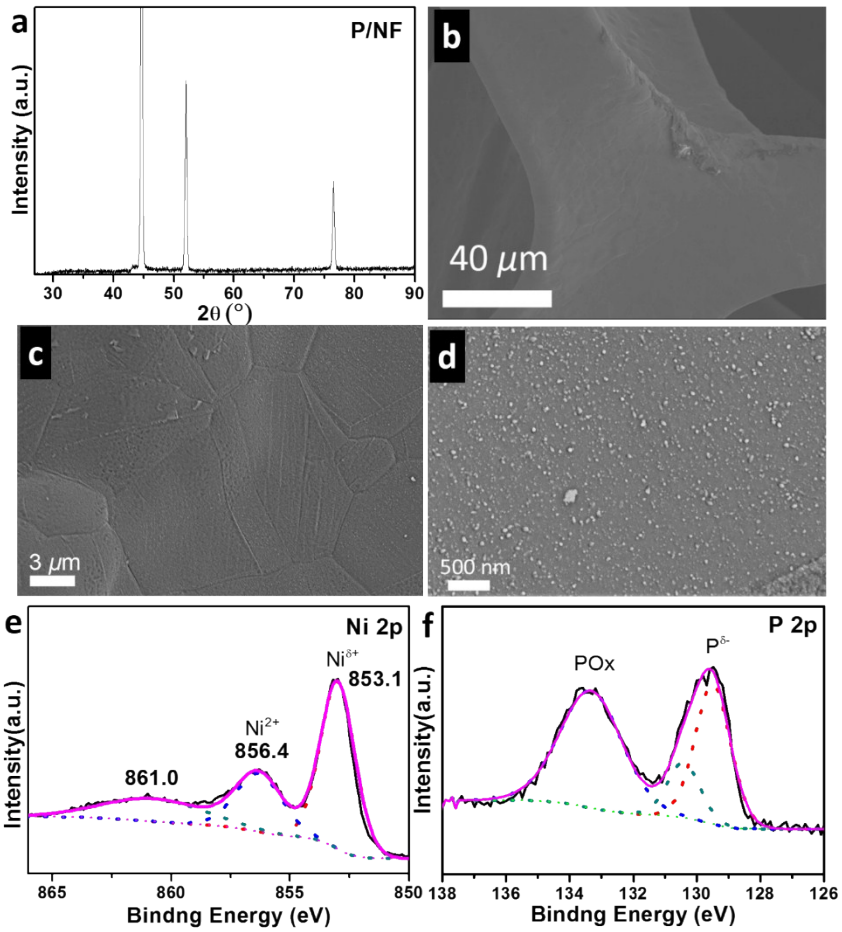

Fig. S5 Direct phosphorization of Ni foam. (a) XRD pattern, (b-d) SEM images, (e-f) XPS spectra.

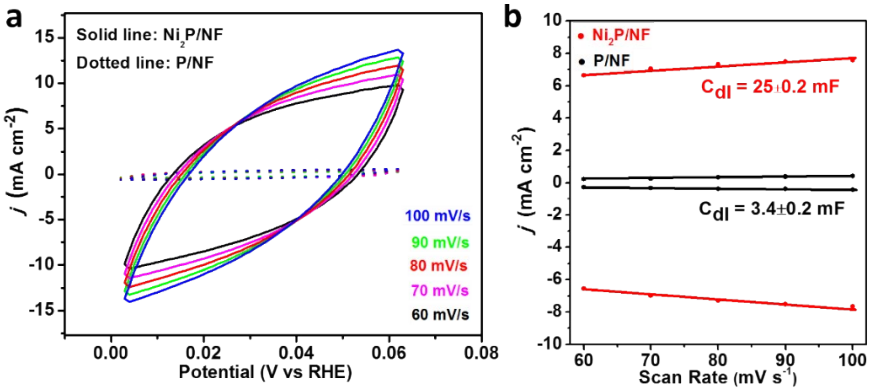

Figure S6. (a) CV curves of Ni_2P/NF and P/NF in the double layer region at scan rates of 60, 70, 80, 90 and 100 mV s^{-1} in 0.5 M H_2SO_4. (b) Current density as a function of scan rate derived from (a).

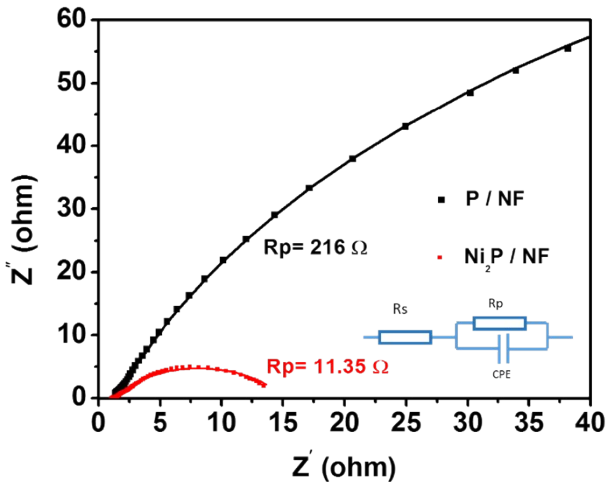

Fig. S7 Electrochemical impedance spectroscopy (EIS). Nyquist plots of the Ni2P/NF and P/F electrode measured in the frequency range of 10^5 – 10^{-2} Hz in 0.5 M H_2SO_4. The data are fitted using the modified Randle equivalent circuit shown in the inset illustration.

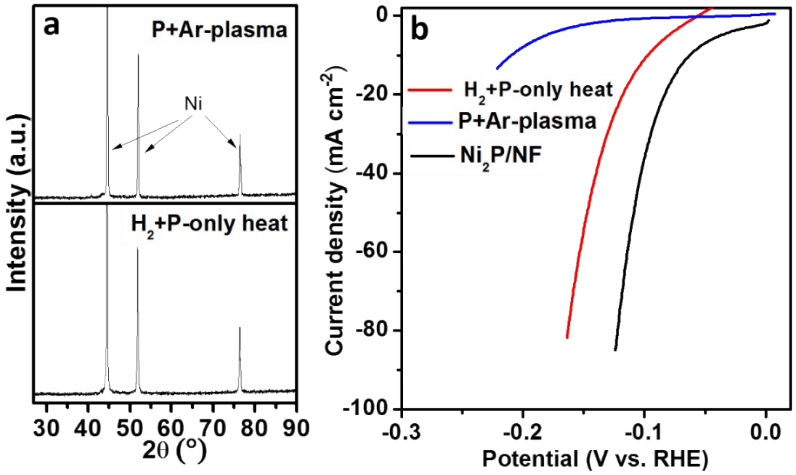

Fig. S8 (a) XRD patterns and (b) linear polarization curves in 0.5 M H_2SO_4 of two controlled samples. Phosphorization in Ar plasma and in Ar/H_2 flow at 250 °C without plasma.

Table S 1 Comparison of the catalytic activity towards the HER in 0.5 M H_2SO_4 of the Ni_2P/NF with other reported catalysts of high HER performance.

Catalyst	Phosphorization temperature (°C)	P source	Loading (mg cm^{-2})	η (mV) at j=10 mA cm^{-2}	Tafel slope (mV dec^{-1})	Ref.
Ni_2P/NF	250	Red P	0.48	65	63	This work
Co-Ni-P/NF	500	Red P	6.0	68	56.4	[1]
CP@Ni-P	500	Red P	25.8	98	58.8	[2]
MoP@PC	850	$(NH_4)_2HPO_4$	0.41	153	66	[3]
Ni_2P@NC	700	$NH_4H_2PO_4$	1.0	138	57	[4]
Ni_2P-Me/GC	700	nickel methylphosphonate $NiO_3PCH_3 \cdot H_2O$	0.42	87	64	[5]
Cu_3P@NPPC-650	250	NaH_2PO_2	0.29	89	76	[6]
Co_2P	370	Triphenylphosphine	1.0	134	71	[7]
Ni_2P	250	NaH_2PO_2	0.38	140	87	[8]
Cu_3P NW/CF	300	NaH_2PO_2	15.2	143	67	[9]
FeP	300-450	$NaH_2PO_2 \cdot H_2O$	0.9	145	65	[10]
mp-Ni_2P/Ni	300	NaH_2PO_2	2	140[a]	68.9	[11]

Note: NF – Ni foam, CP – carbon paper, GC–glassy carbon electrode. NPPC-N,P-codoped carbon shell

[a] overpotential at 20 mA cm^{-2}

Supplementary References

[1] W. Li,D. Xiong,X. Gao,W.-G. Song,F. Xia.L. Liu. *Catal. Today.* 2017**, 287,** 122.

[2] X. Wang,W. Li,D. Xiong,D. Y. Petrovykh.L. Liu. Adv. *Funct. Mater.* 2016, **26**, 4067.

[3] J. Yang, F. Zhang, X. Wang, D. He, G. Wu, Q. Yang, X. Hong, Y. Wu, Y. Li, *Angew. Chem. Int. Ed.* 2016, **55**, 12854.

[4] Z. Pu,C. Zhang,I. S. Amiinu,W. Li,L. Wu.S. Mu. *ACS Appl. Mater. Interfaces.* 2017, **9**, 16187.

[5] R. Zhang,P. A. Russo,M. Feist,P. Amsalem,N. Koch.N. Pinna. *ACS Appl. Mater. Interfaces.* 2017, **9**, 14013.

[6] R. Wang, X. Y. Dong, J. Du, J. Y. Zhao, S. Q. Zang, *Adv. Mater.* 2018, **30**, 1703711.

[7] Z. Huang, Z. Chen, Z. Chen, Z Chen, C. Lv, G. Humphrey, C. Zhang, *Nano Engergy.* 2014, **9**, 373.

[8] L.Feng, H. Vrubel, M. Bensimon, X Hu. *Phys. Chem. Chem. Phys.* 2014, **16**, 5917.

[9] J. Tian, Q. Liu, N. Cheng, A. Asiri, X. Sun. *Angew. Chem. Int. Ed.* 2014, **53**, 9577.

[10] L. Tian, X. Yan, X. Chen. *ACS catal.* 2016, **6**, 5441.

[11] X. Wang, Y. Cao, Y. Teng, H. Chen, Y. Xu, D. Kuang. *ACS Appl. Mater. Interfaces.* 2017, **9**, 32812.